Available online at www.sciencedirect.com
ScienceDirect
Journal of Non-Crystalline Solids 352 (2006) 5453–5462
JOURNAL OF NON-CRYSTALLINE SOLIDS
www.elsevier.com/locate/jnoncrysol

Effects of progressive changes in organoalkoxysilane structure on the gelation and pore structure of templated and non-templated sol–gel materials

Bing Tan [1], Stephen E. Rankin *

Department of Chemical and Materials Engineering, University of Kentucky, Lexington, KY 40506, USA

Received 22 September 2005; received in revised form 17 September 2006

Abstract

We study how progressive changes in silane structure affect the synthesis and properties of organosilicas. Tetraethoxysilane (TEOS), tetramethoxysilane (TMOS), methyltrimethoxysilane (MTMS), bis(trimethoxysilyl)ethane (BTMSE), bis(trimethoxysilyl)hexane (BTMSH), and bis(trimethoxysilylpropyl)amine (BTMSPA) are used as precursors in non-templated base and acid-catalyzed sol–gel processes, and in templated processes with cetyltrimethylammonium bromide (CTAB) and polyoxyethylene 10 lauryl ether ($C_{12}E_{10}$). The gel time of materials made without templates is mainly controlled by the structure of the silane rather than its reactivity. For instance, a dangling methyl group (MTMS) inhibits gelation, while a short bridging chain (BTMSE) promotes gelation. In basic conditions, mesoporous materials are obtained with TEOS and TMOS, while microporous materials are obtained with organically modified silanes without added amine. Dipropylamine, originally added as a catalyst, in fact templates mesopores in BTMSH-derived organosilica. In acidic conditions without pore templates, all products are microporous. In the presence of CTAB, mesopore templating occurs with TEOS, TMOS, BTMSE, and BTMSPA. With $C_{12}E_{10}$, mesopore templating occurs with TEOS, TMOS, and BTMSE. Surprisingly, the BTMSE-based material has the most uniform mesopores of all samples in the $C_{12}E_{10}$ series. Mesopore templating fails when a dangling organic limits the formation of stable pore walls (MTMS) or a large hydrophobic chain disrupts the formation surfactant micelles (BTMSH).

PACS: 81.07.Pr; 81.16.Dn; 81.20.Fw; 81.05.Rm

Keywords: Micelles; Porosity; Nanocomposites; Silicates; Organic–inorganic hybrids; Sol–gels (xerogels); Solution chemistry

1. Introduction

The sol–gel process is an established route to microporous and mesoporous ceramics with high surface areas and pore volumes [1,2]. Because it can be carried out at room temperature, this process allows the incorporation of organic components into nanostructured organic–inorganic hybrid materials [3–7]. One would expect to be able to prepare porous materials with controlled functionality, porosity, and responsiveness to the environment by hydrolytic polycondensation of different alkoxysilanes (Eqs. (1) and (2)). In practice, sol–gel materials often require controlled drying processes (very slow or supercritical drying) to obtain porous materials with high surface areas, and even then the pore size distributions are relatively broad [1]:

$$\equiv\mathrm{SiOR} + \mathrm{H_2O} \xrightarrow{\text{hydrolysis}} \equiv\mathrm{SiOH} + \mathrm{ROH}, \quad (1)$$

$$\equiv\mathrm{SiOH} + \mathrm{HOSi}\equiv \xrightarrow{\text{condensation}} \equiv\mathrm{SiOSi}\equiv + \mathrm{H_2O}, \quad (2)$$

$$\equiv\mathrm{SiOH} + \mathrm{OH^-} \xrightarrow{\text{deprotonation}} \equiv\mathrm{SiO^-} + \mathrm{H_2O}. \quad (3)$$

* Corresponding author. Tel.: +1 859 257 9799; fax: +1 859 323 1929.
E-mail address: srankin@engr.uky.edu (S.E. Rankin).
[1] Present address: Department of Chemistry, Ohio State University, 100 W. 18th Avenue, Columbus, OH 43210, USA.

0022-3093/$ - see front matter © 2006 Elsevier B.V. All rights reserved.
doi:10.1016/j.jnoncrysol.2006.09.026

Beginning with reports by Kresge and co-workers in 1992, the surfactant templated sol–gel process has been widely utilized as a way of making porous materials with well-defined porosity [8–11]. A variety of templating agents can be incorporated into a sol prior to gelation which will be incorporated into the product as non-covalently bound organics. Removal of the templates after gelation generates pores with better size and structure control than the pores normally formed in ceramic gels. Cationic and non-ionic surfactants are the most common templates used to make ordered mesoporous materials. With cationic surfactants, basic conditions are used to promote the formation of deprotonated silanols (Eq. (3)) which co-assemble with the surfactant through electrostatic interactions [12–14]. Under these conditions, the hydrolysis reaction (Eq. (1)) is expected to be the rate-limiting step [1]. Precipitation of co-assembled particles occurs when a sufficient concentration of the nucleating species develops, as dictated by the kinetics of hydrolysis. Differences in the properties of products made from different precursors would therefore be expected to be related either to differences in the kinetics of hydrolysis, or to differences in the structures of the precursors. On the other hand, in the non-ionic surfactant-templated process [15], the precursor is usually hydrolyzed for some of the time in acidic solution (pH $\approx$ 2). During this step, hydrolysis proceeds until it reaches equilibrium but condensation is rate limiting. Conditions can be selected to limit the extent of condensation (Eq. (2)), since the rate of this reaction is minimized at pH 2.0 [1]. To induce rapid condensation and precipitation, a second step is often used in which a base or NaF is added as a catalyst. By using the two-step procedure, hydrolysis and condensation reactions can be independently controlled. However, because hydrolysis proceeds to a large extent in the first step, similar surfactant–precursor interactions are expected for most precursors, so differences in kinetics are expected to have less effect on the product pore structures than the structure and functionality of the precursor (especially the type and arrangement of non-hydrolyzable functional groups).

In addition to non-covalently bound pore templates, the sol–gel method allows the incorporation of covalently bound organics through the use of organically modified alkoxysilane precursors. The organic groups in these precursors can be classified as non-bridging (dangling organics) or bridging (an organic group bridging two trialkoxysilyl sites). The organic groups impart specific functionality to the hybrid material, and mixtures of organoalkoxysilanes can be used to prepare multifunctional or stimulus-responsive materials [16,17]. Bridged silanes with various types of bridging chains have been used to make porous materials in both non-templated and templated sol–gel processes [3,6,7]. In the non-templated process, the dried products normally have large surface areas only when they are prepared in basic conditions [3]. Under acidic conditions, the materials are more elastic and they tend to collapse during drying [3,18]. In the templated sol–gel process, stiff bridging organics such as ethylene, acetylene, phenylene and polyphenylene groups have been used to make ordered materials [6,7,19–21]. However, no material with a narrow pore size distribution (PSD) has been synthesized using a silane with long flexible chain (>C5) as the sole precursor, presumably because the flexible bridging chains make the material too soft to withstand drying stresses after the removal of the pore template.

Here, we systematically investigate a series of materials prepared using the series of silanes whose early-stage reaction kinetics we have measured [22]. The precursors (Fig. 1) include tetralkoxysilanes and alkoxysilanes with a dangling methyl group, a bridging ethylene group, a bridging hexylene chain, and a bridging amine-functional chain. Materials are prepared in the absence of a surfactant under acidic or basic conditions, and using either the cationic surfactant cetyltrimethylammonium bromide (CTAB) or the non-ionic surfactant polyoxyethylene 10 lauryl ether ($C_{12}E_{10}$) as the pore template. The results are interpreted

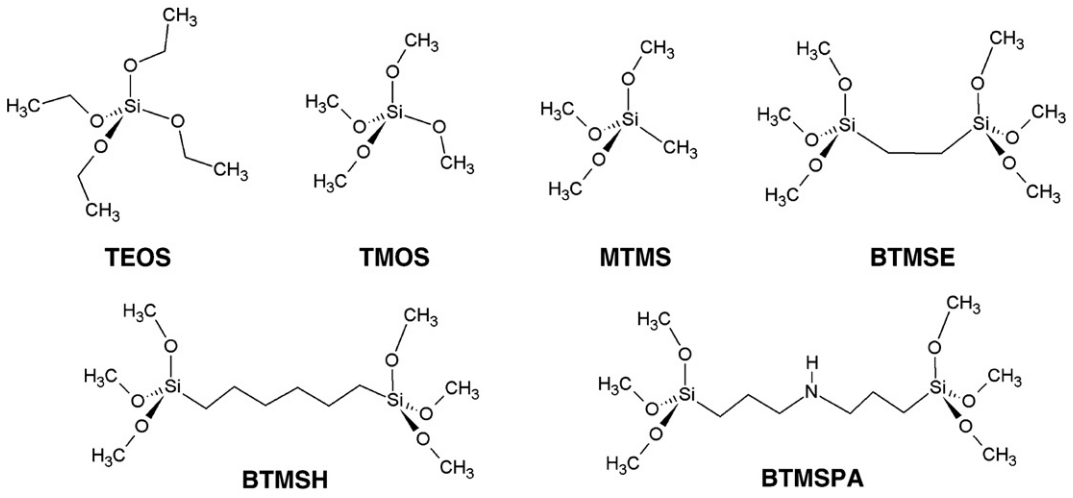

Fig. 1. The set of precursors used for this investigation.

based on what would have been expected from the kinetic trends for the hydrolysis and condensation reactions of the precursors, and on the structures of the precursors. This series of precursors highlights the influence of gradual changes in precursor structure on the pore properties of the products, especially the roles of precursor structure in network formation and co-assembly.

2. Experimental

2.1. Materials

Tetraethoxysilane (TEOS, 99+%), tetramethoxysilane (TMOS, 99+%), methyltrimethoxysilane (MTMS), bis (trimethoxysilyl)ethane (BTMSE, 95+%), bis(trimethoxysilyl) hexane (BTMSH), and bis(trimethoxysilylpropyl) amine (BTMSPA, 95%) were purchased from Gelest. CTAB (99%) and $C_{12}E_{10}$ were purchased from Sigma. The solvents and reagents used were deionized ultrafiltered water (Fisher Scientific), anhydrous ethanol (Aaper Alcohol and Chemical), HPLC grade methanol (Fisher), concentrated aqueous HCl (36.5%, Fisher), and NaF (technical grade, MCB). All chemicals were used as received.

2.2. Non-templated samples

To prepare the sol–gel materials, two solutions were initially prepared, one containing the precursor in dry methanol, and the other containing water and acid or base in methanol. The solutions were mixed together and the time was recorded.

Seven base-catalyzed samples (B1–B7) were prepared with the same molar compositions but with the precursors being TEOS, TMOS, MTMS, BTMSE, BTMSH, BTMSH, or BTMSPA, respectively. The initial molar ratios were 1 $SiOCH_3$ ($SiOCH_2CH_3$ with TEOS):1 H_2O:20 methanol:0.018 NaOH:x dipropylamine ($x = 0.17$ for sample B6, $x = 0$ for the others). Samples B6 and B7 were prepared to compare the effect of an amine external to the bridging chain of BTMSH (B6), or integral in the bridging chain of BTMSPA (B7).

Five samples (A1–A5) were prepared under acidic conditions with the same series of precursors: TEOS, TMOS, MTMS, BTMSE, and BTMSH, respectively. The molar ratio of $SiOCH_3$ ($SiOCH_2CH_3$ with TEOS):H_2O:HCl: methanol for all samples in this series (A1–A5) was 1:1:0.018:6.8. Samples A6 and A7 were again prepared to compare the effect of the amine external to BTMSH or integral within the bridging chain of BTMSPA. However, to make the solutions acidic, an excess of HCl was added beyond the quantity of amine present. In sample A6 (BTMSH), a quantity of dipropylamine was added comparable to the amount of amine in sample A7 (BTMSPA). The initial molar ratios of $SiOCH_3$:H_2O:HCl:dipropylamine:methanol were 1:1:0.185:x:12.7 ($x = 0.167$ for B6, $x = 0$ for B7) in samples B6 and B7.

All solutions were prepared in sealed polystyrene vials. The solutions were aged at room temperature until the gel point, which we defined as the time when no movement of the meniscus of the sample could be observed within one minute of tilting the vial at 45° from vertical.

2.3. CTAB templated samples

The procedure to prepare CTAB-templated materials was based on the procedure of Kumar et al. [23] CTAB, water, and concentrated ammonia were stirred together for 10 min before the dropwise addition of the precursor. After adding all ingredients, the solution was aged at room temperature for 24 h with stirring. The solution was then filtered and the as-synthesized sample was dried in air overnight. The surfactant was subsequently removed by washing/ion exchange with acidic ethanol (5 ml 36.5 wt% HCl in 150 ml ethanol). Six CTAB-containing samples (C1–C6) were prepared with the same molar compositions (1 $SiOCH_3$ ($SiOCH_2CH_3$):0.13 CTAB:2.4 NH_3:138 H_2O) but with different precursors (TEOS, TMOS, MTMS, BTMSE, BTSH, and BTMSPA, respectively).

2.4. PEO-based non-ionic surfactant templated samples

The procedure for preparing $C_{12}E_{10}$-templated materials was similar to the procedure reported by Bossiere et al. [24] $C_{12}E_{10}$, water, and HCl were first mixed together with stirring, followed by addition of the precursor. After aging at room temperature for one day, the desired amount of solid NaF was added to the solution. The solution was then aged at 55 °C for 3 days with stirring. The solution was filtered and the $C_{12}E_{10}$ was removed from the sample by Soxhlet extraction with 150 ml of ethanol. Five samples (N1–N5, with TEOS, TMOS, MTMS, BTMSE, and BTMSH as precursors, respectively) were prepared with the molar composition of 1 $SiOCH_3$ ($SiOCH_2CH_3$):0.12 $C_{12}E_{10}$: 0.059 HCl:329 H_2O:x NaF ($x = 0.06$ for samples N1, N2, N4, and N5; $x = 0.60$ for sample N3). Because of the amine in BTMSPA, an excess of acid was added to sample N6; its molar composition was 1 $SiOCH_3$:0.12 $C_{12}E_{10}$:0.68 HCl:329 H_2O:0.60 NaF.

2.5. Characterization

Powder X-ray diffraction (XRD) patterns of the products were recorded in the Bragg–Brentano geometry using a Siemens 5000 diffractometer by scanning 2θ at a rate of 0.1°/min from 1.5° to 7.5° in increments of 0.02°. We utilized 0.15406 nm Cu K_α radiation and a graphite monochromator for XRD. Nitrogen sorption was measured at 77 K with a Micromeritics Tristar 3000 automated nitrogen adsorption apparatus. Samples were degassed under flowing nitrogen at 120 °C for over 4 h before the measurement. The KJS modified BJH method [25,26] was used to estimate the PSDs of all samples.

3. Results and discussion

3.1. Comparison of products made by the non-templated base catalyzed sol–gel process

Seven samples (B1–B7) were prepared under basic conditions. Hydrolysis rate coefficients (k_h), gel times and product properties of these samples are compared in Table 1. From our study of the sol–gel kinetics of these precursors [22], we know that the k_h values in basic conditions of TMOS, MTMS, and BTMSE are similar in magnitude, while the k_h values of BTMSH and TEOS are similar to each other, and almost an order of magnitude lower than the others. Gel times measured for this series of samples (Table 1) seldom follow the trends that would have been expected based on the differences in k_h. The gel times and reactivities follow the expected relationship only for samples B1 and B2. TEOS is less reactive than TMOS and, as expected, the gel time of B1 is longer than that of B2. However, because transesterification plays an important role in sample B1 [22], the difference in the gel times is not as large as would be expected based on the difference in k_h.

The expected inverse correlation between kinetics and gelation time for samples B2–B4 is not found. While MTMS and BTMSE have similar k_h values to TMOS, TMOS took many months to form a gel compared to only several days for formation of a precipitate for sample B3, and a gel for sample B4. The large difference in the gel times cannot be explained directly by the k_h trends. This difference also is larger than would be predicted based on differences in the number of polymerizable functional groups on each monomer; assuming second-order kinetics [22] and random branching theory for gel conversions [27], the gel time ratio would be predicted to be roughly 2:4:1 for samples B2–B4, respectively. This does not match the experimental trend.

The reason for slow gelation of TEOS and TMOS is most likely the formation of cage-like silsesquioxane structures or siloxane rings [28]. When these structures form, gelation happens at a much higher overall conversion than is predicted by random branching theory, and the cages or rings interconnect into a three-dimensional network structure very slowly [28–32]. When one of the alkoxy groups of TMOS is replaced with $-CH_3$ to form MTMS, cage-like nanoparticles would still be expected to form, but their solubility is limited [33–35]. When the concentration of cages or rings is large enough, they will crystallize or precipitate from the solution. When BTMSE is used instead of MTMS, the siloxane cages or rings initially formed are easily connected to each other because of the pre-existing ethylene bridges. A three-dimensional network structure is therefore more easily formed than with TMOS or TEOS. Thus, we conclude that structural effects due to the arrangement of non-hydrolyzable organic groups best explain the differences in gel times among samples B2–B4.

Comparing samples B4 and B5, the k_h value of BTMSE exceeds that of BTMSH by almost an order of magnitude [22], yet the gel time of BTMSE is significantly larger. However, the products do not look the same. While the BTMSE gel is transparent, the BTMSH gel is opaque, indicating phase separation. Since the bridging chain is short in sample B4 (ethylene), the sol remains homogeneous and transparent until gelation. A long, hydrophobic bridging chain (hexylene) causes phase separation to occur during the polymerization process of B5 which may accelerate the gelation of BTMSH. An additional reason that BTMSH gels more quickly than BTMSE is that ethylene-bridged silanes are capable of forming 5-atom carbosiloxane rings which delay gelation [36]. Hexylene-bridged silanes do not readily form carbosiloxane rings, so gelation can occur without interference from cyclization. Linear and branched chains composed of alkylene groups and small siloxane clusters should be favored by a long bridging chain.

BTMSPA has six carbon atoms and one amine group in the bridging chain, which is slightly longer than that of BTMSH, but because of the amine, the k_h value of BTMSPA is much larger than that of BTMSH [22]. Surprisingly, the gel time of BTMSPA (sample B7) is also much longer than that of BTMSH under the same conditions (B5). The reason is most likely the increased hydrophilicity of the bridging chain in BTMSPA. The amine group helps to keep the growing carbosiloxane polymers in solution, leading to the slow formation of a homogeneous, transparent gel. Sample B6 rules out the possibility that the difference in gelation times is simply due to an inhibiting effect of the amine. When the amine is absent from the bridging chain but an equivalent amount of dipropylamine is present (sample B6), the hydrolysis kinetics and gel time are similar to those of the hexylene-bridged sample without dipropylamine (B5).

Table 1
Kinetics of formation and characteristics of products of sol–gel reaction in basic conditions

Sample	Precursor	k_{h1}[a] ($M^{-1}\,s^{-1}$)	Gel time	Product morphology	S_{BET} (m^2/g)
B1	TEOS	0.293 ± 0.004	6 months	Transparent gel	401
B2	TMOS	2.35 ± 0.03	5 months	Transparent gel	428
B3	MTMS	1.97 ± 0.01	–	Particles	261
B4	BTMSE	2.69 ± 0.03	72 h	Transparent gel	727
B5	BTMSH	0.305 ± 0.004	2.5 h	Opaque gel	106
B6	BTMSH	0.369 ± 0.007	2 h	White powder	254
B7	BTMSPA	1.54 ± 0.02	18 h	Transparent gel	88

[a] First hydrolysis rate coefficients for the precursors in methanol at 22 °C [22].

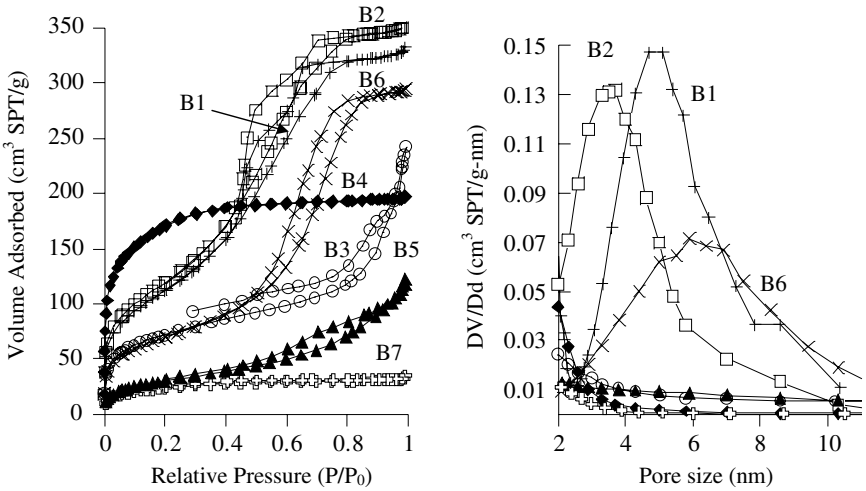

Fig. 2. Nitrogen sorption isotherm plots and pore size distributions for samples B1, B2, B4, B5, B6, and B7.

Nitrogen adsorption isotherms of the products obtained after drying are compared in Fig. 2. The isotherm type varies widely but can be explained based on gel time and monomer structure trends. Samples B1 and B2 have type IV isotherms with triangular hysteresis loops typical of silica xerogels with broad imhogeneous mesopore size distributions (Fig. 2) [37]. Sample B3 has a low surface area (Table 1) and a type II adsorption isotherm with a H3 hysteresis loop [37]. The hysteresis loop does not close at low relative pressure due to an artifact caused by the small surface area of the sample. This isotherm is consistent with a sample consisting of aggregates of nanoparticles with little internal porosity formed by precipitation of the MTMS product. Sample B5 has similar characteristics to B3 because BTMSH undergoes precipitation during gelation. In contrast, the rigidity of BTMSE allows a large surface area to be retained in sample B4, although the type I isotherm indicates that it is microporous [37]. Sample B7 also has a type I isotherm, but a low surface area. The homogeneous, soft elastic network formed by BTMSPA in B7 is able to collapse during drying [38]. Sample B6 is surprising because, while it is made with the same precursor as B5, it has an inflection and hysteresis loop indicating mesoporosity. In this case, dipropylamine most likely acts as a mesopore template. Thus, we find that precursors that form rigid networks (B1, B2 and B4) and samples with pore templates (B6) retain the highest porosity in this series. Samples B3 and B5 have low surface areas because they are composed of particles. Sample B5 also may undergo collapse during drying in ambient conditions rather than with a low surface tension fluid [3]. Sample B7 forms a homogeneous soft gel which collapses during drying.

3.2. Comparison of products made by the non-templated acid-catalyzed sol–gel process

Seven samples (A1–A7) were prepared in acidic conditions without surfactants. pH values in the solutions should have been the same assuming that all of the amines in samples A6 and A7 were titrated by HCl (this was confirmed in our kinetic study [22]). Gel times and total surface areas of all samples are compared in Table 2.

As in basic conditions (Table 1), transparent homogeneous gels formed in samples prepared from TEOS, TMOS, BTMSE, and BTMSPA. This indicates that the growing siloxane polymers from those precursors remained soluble during polymerization. In contrast, the samples prepared from MTMS and BTMSH were inhomogeneous. The trend in the gel times was similar to that found in basic conditions. A1 had a similar gel time to A2 because of the transesterification reaction. Because of limited solubility of the methyl groups, dense particles precipitated with MTMS as the precursor (A3). A4 gelled much faster than A2 because of the pre-existing bridging ethylene chain. With an increase of the alkylene chain length, the gel time was much shorter, but an inhomogeneous product was obtained (A5). The reactants in sample A6 were more dilute than those in sample A5. This may cause the difference in the gel times between A5 and A6. It took much longer time for sample A7 to gel than sample A6. Because the kinetics of condensation of BTMSH and BTMSPA under acidic conditions are of the same magnitude [22], the difference in gel times is best explained by poor solubility of the hexylene bridge (A6) compared to the amine-containing bridge (A7).

Nitrogen isotherms of the acid-catalyzed non-templated samples are shown in Fig. 3. Samples A1, A2, A4, and A5 have type I adsorption isotherms and are microporous. Microporous xerogels are typically produced by acid-catalyzed alkoxysilane hydrolysis [1]. Because of the flexibility of the hexylene chain, sample A6 is virtually non-porous. The surface area of sample A7 is also very low. However, sample A7 has a type IV adsorption isotherm with a H2 hysteresis loop consistent with a narrow PSD (Fig. 3). Like the samples prepared under basic conditions, the total surface area decreases as the bridging alkylene chain length increases.

Table 2
Formation kinetics and characteristics of products of sol–gel reaction in acidic conditions

Sample	Precursor	k_{ac}[a] ($M^{-1}\,s^{-1}$)	Gel time	Product morphology	S_{BET} (m^2/g)
A1	TEOS	–	8 months	Transparent gel	410
A2	TMOS	1.08 ± 0.09	7 months	Transparent gel	500
A3	MTMS	3.6 ± 0.2	–	Few particles	–
A4	BTMSE	1.05 ± 0.07	60 h	Transparent gel	685
A5	BTMSH	0.18 ± 0.05	22 min	Opaque gel	240
A6	BTMSH	0.41 ± 0.01	20 h	Opaque gel	2
A7	BTMSPA	0.22 ± 0.01	17 days	Transparent gel	37

[a] Water-producing condensation rate coefficients for the precursors in methanol at 22 °C [22].

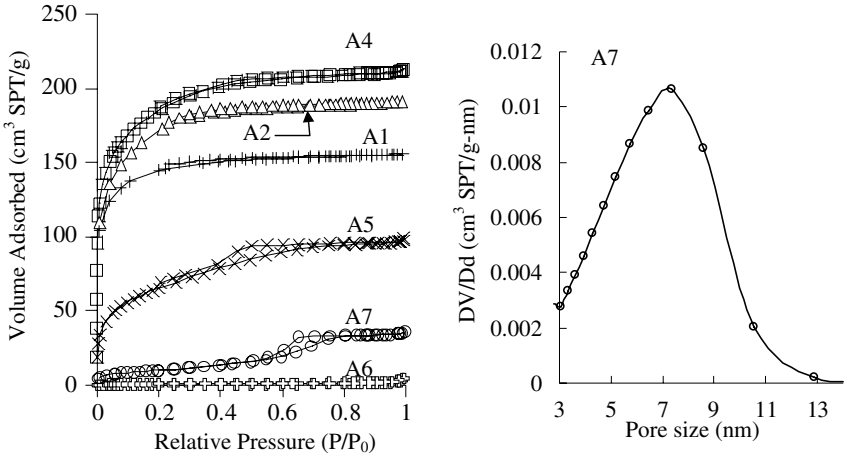

Fig. 3. Nitrogen sorption data: isotherms for samples A1, A2, A4, A5, A6 and A7 and pore size distribution of sample A7.

To summarize the non-templated samples prepared in either acidic or basic methanol, both TEOS or TMOS slowly form homogeneous, transparent gels which can be dried to form xerogels consistent with previous reports [1]. The methyl group of MTMS promotes precipitation rather than gelation because low molecular weight silsesquioxanes accumulate. The stiff bridging chain of BTMSE allows rapid formation of gels that are stable to drying. Thus, BTMSE can be used as an organically modified substitute for TEOS or TMOS in circumstances when rapid gelation is desirable. Extending the organic bridge in BTMSH produces materials that are unstable to rapid ambient drying (although materials with a surface area of 560 m^2/g can be prepared by careful drying [3]). Adding a hydrophilic amine group to the organic bridge, in BTMSPA, allows homogeneous gels to form, but they are susceptible to collapse upon drying. The hydrophilic, basic amines in BTMSPA-derived samples may also reduce their stability.

3.3. Comparison of products made by a cationic surfactant-templated sol–gel process

The CTAB templated sol–gel process in basic solution is a common process used to make ordered mesoporous materials, such as MCM-41 [23,39]. As discussed in Section 1, cationic surfactant templating is usually performed in basic conditions, and electrostatic attraction results in precipitation of dense aggregates of surfactant and the hydrolyzed precursor [40]. The local density of silica species in the precipitated phase should be much higher than in non-templated sol–gel systems, which is expected to increase the condensation rate dramatically. However, condensation can occur in either the bulk phase or in precipitated particles. Condensation in the absence of templates will be called 'bulk condensation' in this paper to distinguish it from localized condensation occurring among the species co-assembled with templates.

The measured properties of all samples are shown in Table 3. Solutions of samples C1–C4 became turbid within several minutes after adding the precursor. For C6 (with BTMSPA), a large amount of precipitates formed quickly. For comparison, a solution was prepared under the same conditions as C2 (with TEOS as the precursor) but without CTAB, and no gel or precipitate was obtained after several days. This indicates that localized condensation is dominant over bulk condensation in the precipitated particles. After aging, these products remained powders. In contrast, a gel formed immediately after adding BTMSH to sample C5, and was retained after aging. Formation and gelation of a three-dimensional network structure suggests that bulk condensation was important for sample C5.

Table 3
Characteristics of products prepared with CTAB as the template

Sample	Precursor	As-synthesized product morphology	Product weight (g)	d_{100} (nm)	S_{BET} (m^2/g)	Pore size (nm)
C1	TEOS	White powder	0.51	3.53	853	3.5
C2	TMOS	White powder	0.48	3.40	922	3.4
C3	MTMS	White powder	0.60	–	696	–
C4	BTMSE	White powder	0.76	3.71	1214	3.1
C5	BTMSH	Gel	0.99	–	475	–
C6	BTMSPA	White powder	1.44	5.52	358	3.1

The nitrogen sorption isotherms of all CTAB-templated samples are shown in Fig. 4. In spite of the slower hydrolysis rate of TEOS compared to TMOS [22], C1 and C2 precipitated at about the same time, and both samples have reversible type IV isotherms and narrow PSDs similar to MCM-41 [8,9]. Thus, hydrolysis kinetics have a negligible effect on product properties in this case, perhaps due to the dominance of localized condensation near CTAB micelles. The replacement of one methoxy group with a methyl group in MTMS (sample C3) disrupts the interactions with CTAB and the formation of a network in the pore walls. Therefore, the surface area is reduced, the pores are expanded, and the uniformity of the pores is less than in C1 and C2 (indicated by the large hysteresis loop in Fig. 4). In contrast, the rigid ethylene bridge of BTMSE (sample C4) allows a well-connected network to form, leading to a product similar to C1 and C2, but with a slightly broader PSD. The situation changes with BTMSH as the precursor (C5). The hexylene bridging chain is long, flexible, and hydrophobic. The sample gels because bulk condensation can easily proceed even in the presence of CTAB. The hysteresis loop in the isotherm of this sample (Fig. 4) indicates poor micelle templating, probably because mixing of hexylene bridges with the tails of CTAB discourages the formation of ordered aggregates. Adding an amine to the bridging chain (with BTMSPA, sample C6) allows a narrow pore size distribution to again be obtained (inset of Fig. 4). The amine group in the bridging chain may help to attract the surfactant headgroups through hydrogen bonding, or to reduce the favorable interactions between the surfactant tail and the bridging chain. The large yield of precipitates and the narrow mesopore size distribution of C6 indicate that CTAB associates well with BTMSPA. Because of their bridging organics, the organosilica samples with ordered pores (C4 and C6) have a slightly smaller pore size than the silica samples (C1 and C2).

The long-range order of the pores of all samples was characterized by XRD. Samples C1 and C2 have typical 2D hexagonal structures (not shown). The XRD patterns of C4 and C6 each have only one sharp reflection consistent with wormhole-like/disordered hexagonal pores. Sample C6 is the first reported material that we are aware of with uniform wormhole-like mesopores made with BTMSPA as the sole precursor [16,17]. XRD patterns of C3 and C5 do not show reflections, which is consistent with the absence of narrowly distributed pores in the nitrogen adsorption isotherms. The d_{100} spacing (Table 3) of C6 is much larger than that of C4, which is again larger than that of C2/C1. Since the pore sizes of C4 and C6 are the same (slightly smaller than C2), we can infer that the incorporation of a bridging chain increases the pore wall thickness, and that longer bridging chains give thicker pore walls in CTAB-templated materials.

The investigation of CTAB templating shows that most of the precursors co-assemble with CTAB to form ordered mesoporous materials. Only samples C3 and C5 have no long-range ordering and broad non-uniform PSDs. The

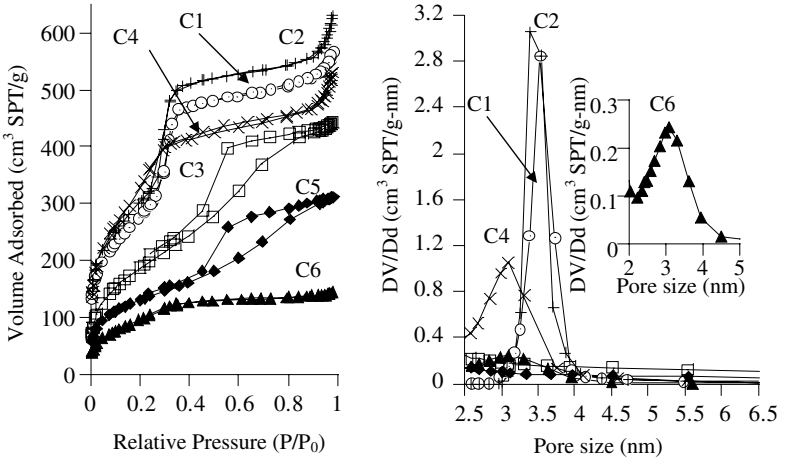

Fig. 4. Nitrogen sorption isotherm plots and pore size distributions for samples C1–C6.

reasons are most easily related to the structures of the precursors rather than to reaction kinetics. In sample C3, the single alkyl modifier of MTMS limits the formation of solid walls that are stable during removal of the surfactant. The poorly connected structure of MTMS/CTAB aggregates is illustrated with another sample prepared with almost the same composition as C3, but with only half of the MTMS. Poor yield (less than 0.02 g compared with >0.2 g for the others) and the light, flaky texture of the as-prepared product suggest weak wall connectivity. The long, hydrophobic bridging chain of BTMSH is most likely to be the reason for poor ordering in sample C5. The long bridging chain facilitates bulk condensation. However, the lack of mesopores is not only a result of the bridging chain length; uniform mesopores are found in the product made with BTMSPA (C6). The hydrophobic chain of BTMSH also can interact with the tails of CTAB through dipolar and hydrophobic forces, thus disrupting the formation of the silica/surfactant aggregates. Although both C3 and C5 lack narrow PSDs, their surface areas are still much higher than the materials made without a surfactant (B3 and B5), which indicates that CTAB helps to form or stabilize pores. When BTMSPA is used, the hydrophilic chain helps to promote co-assembly of the precursor with CTAB micelles, thus limiting bulk condensation. Templating is indicated by the presence of narrowly distributed mesopores (inset of Fig. 4) and a larger surface area than the samples obtained by the non-templated sol–gel processes (A7 and B7). The low specific surface area of C6 compared to C1 and C2 may be simply because the sample has thicker pore walls. Although it does not have an extremely high specific pore volume, sample C6 has a combination of uniform mesoporosity and integral amines in the pore walls that is ideal for selective basic catalysis, adsorption, and for further functionalization.

3.4. Comparison of products made by the non-ionic surfactant-templated sol–gel process

Non-ionic polymeric surfactants can be prepared in a very wide array of molecular weights, so a wide variety of large pores can be created which are useful for applications such as protein adsorption [41–43]. Thus, there is significant incentive to compare the non-ionic templating process to templating with cationic surfactants.

As discussed in Section 1, the co-assembly of non-ionic surfactants such as $C_{12}E_{10}$ with hydrolyzed silanes is driven by hydrogen bonding rather than electrostatic interactions [44]. The acidic first hydrolysis step used for non-ionic surfactant templating creates a high concentration of silanol groups [15] for all precursors. We hypothesize that rapid condensation induced by NaF addition in the second step [24] should make the product structure more dependent on precursor structure than on the rate coefficients of the sol–gel reactions.

Properties of samples N1–N6 are compared in Table 4. Before the addition of NaF, all solutions were aged for 1 day at room temperature. The precursors are expected to be completely hydrolyzed since the hydrolysis reaction is very fast in acidic conditions [45]. Condensation is expected to happen to some extent during this step, although it should be slow. Weakly condensed silica/PEO aggregates remain soluble if they have enough –OH groups. However, the dangling methyl groups of MTMS cause the formation of a turbid solution for sample N3 prior to the addition of NaF. The long hydrophobic chain of BTMSH also limits the solubility of $C_{12}E_{10}$/hydrolyzed BTMSH aggregates. Moreover, the long bridging chain of BTMSH allows these weakly condensed structures to form gelatinous particles during hydrolysis. All other precursors (TEOS, TMOS, BTMSE and BTMSPA) remained soluble during the acidic hydrolysis step.

Upon the addition of a small amount of sodium fluoride (NaF/Si = 0.06), precipitates were observed for TEOS, TMOS, BTMSE, and BTMSH. No precipitates were observed for MTMS or BTMSPA after 3 days. BTMSPA has a hydrophilic chain which helps to dissolve the condensed material, and while the MTMS solution was turbid after the acid step, the methyl groups of MTMS prevented large-scale precipitation. Increasing the amount of NaF to 0.6 NaF/Si was required to obtain precipitates for BTMSPA and MTMS.

Isotherm plots and PSDs of the N-series samples are compared in Fig. 5. Samples N1 and N2 have similar type IV isotherms with hysteresis loops and sharp inflections corresponding to the same pore size. Sample N3, prepared with MTMS, has very low porosity either because of poor interactions between $C_{12}E_{10}$ and the methyl groups or because of the poor network-forming ability of MTMS. The reversible type IV isotherm of N4 indicates a highly

Table 4
Characteristics of products prepared with $C_{12}E_{10}$ as the template

Sample	Precursor	Solution before adding NaF	Weight of extracted sample (g)	d_{100} (nm)	S_{BET} (m^2/g)	Pore size (nm)
N1	TEOS	Clear	0.15	5.38	732	4.3
N2	TMOS	Clear	0.15	5.07	879	4.3
N3[a]	MTMS	Turbid	0.07	–	74	–
N4	BTMSE	Clear	0.14	–	892	3.3
N5	BTMSH	Soft gel precip.	0.31	–	409	–
N6[a]	BTMSPA	Clear	0.44	–	163	–

[a] NaF/Si = 0.60 in samples N3 and N6.

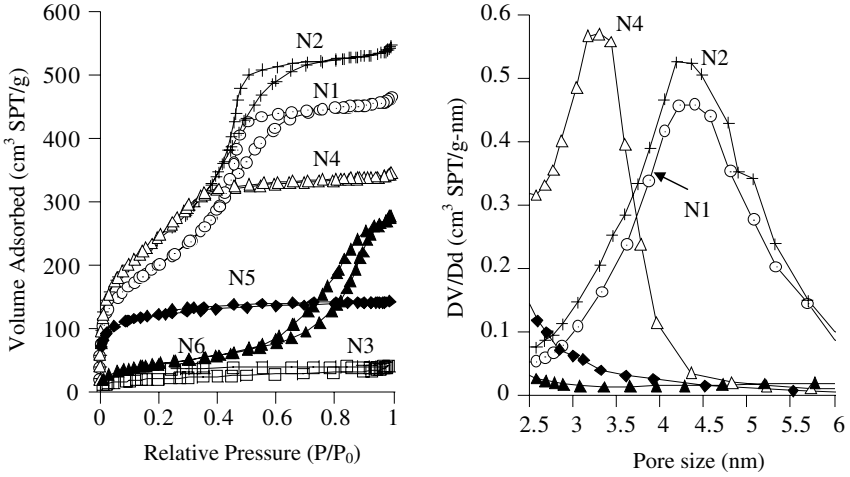

Fig. 5. Nitrogen sorption isotherm plots and pore size distributions for samples N1–N6.

uniform mesopore structure. N5 has a surface area similar to C5, but it does not have any mesopores. Both surface areas are much higher than what would have been obtained without any template (samples B5 and A5). However, all the samples made with BTMSH without adding dipropylamine lack a narrow PSD. The sample prepared with BTMSPA (N6) has a small surface area, but a broad distribution of large mesopores indicated by capillary condensation at high P/P_0.

XRD patterns of samples N1 and N2 only have one sharp reflection (not shown), which indicates that both samples have wormhole-like pore structures. No peak is observed for sample N4, which is possibly because the reflection is out of the range of the XRD instrument (only reflections at >1.5° can be observed). No reflections are observed for samples N3, N5 and N6, as expected from their lack of uniform pores.

The results for the $C_{12}E_{10}$ templated series can, as hypothesized, be explained mainly by the structure of the precursor. The products formed with TMOS and TEOS as the precursor are nearly identical. Both non-bridging methyl-functional precursors prevent network formation, and poor templating with $C_{12}E_{10}$ results. Long bridging chains are also not able to make mesporous materials with narrow PSDs with the non-ionic surfactant $C_{12}E_{10}$ because of both the flexibility of the network and a reduction in the driving force for ordered surfactant/precursor co-assembly. BTMSE appears to have the optimal combination of connectivity and interactions with the surfactant needed to form a templated material, and forms a material with the narrowest mesopore size distribution and the largest specific surface area of this series of samples.

4. Conclusions

Six silanes were used to investigate effects of small, systematic change in the precursor structure on the gel times and product properties of materials prepared with and without pore templates. The gel times in the non-templated sol–gel processes depend more on the structure of the precursor than on the reactivities measured [22] at the start of the reaction. Tetrafunctional silanes gel slowly because of their tendency to form cage-like precursor prior to gelation. A long bridging alkylene chain favors rapid gel formation, although precipitation may occur. Ethylene-bridged silanes and amine-containing bridged silanes gel on a longer time scale, but they tend to remain dissolved in solution until the gel point or until they co-assemble with pore templates.

The materials made with TMOS and TEOS here are similar to each other because of transesterification with the solvent, methanol, and their products conform to expectations. The pores of the products are disordered and mesoporous in basic conditions, microporous in acid, hexagonal close-packed cylindrical mesopores with CTAB, and wormhole-like mesopores with $C_{12}E_{10}$. Adding a methyl group to the precursor (MTMS) prevents good network formation under acidic conditions either without a template, or with $C_{12}E_{10}$. This is due to the prevalence of siloxane cyclization in acidic solutions. Under basic conditions, particles with disordered pores are formed, although CTAB templating increases the surface area. Other precursors with dangling organics are also likely to produce poorly structured materials, especially if they are prone to forming cage-like silsesquioxanes.

Connecting two trimethoxysilane groups with a short ethylene group allows the precursor to gel even more quickly than the tetrafunctional precursors do. The ethylene bridge is stiff enough to allow stable porous materials to form. BTMSE forms high surface area, microporous xerogels in acidic or basic conditions without surfactants. Mesopore templating with either CTAB or $C_{12}E_{10}$ is effective because of the excellent network-forming ability and polarity of BTMSE. Increasing the length of the bridging chain to hexylene allows even more rapid gelation, but the products are inhomogeneous and mostly microporous,

even with a surfactant template. Surfactant templating is not effective because long non-polar alkylene chains reduce the driving force for co-assembly. However, the surfactant still reduces the level of uncontrolled shrinkage during drying, leading to an increase in surface area of the material.

Introducing an amine into the briding chain (with BTMSPA) allows a homogeneous gel to form, but the pores collapse during drying without surfactant templates. The amine also enables CTAB to co-assemble with BTMSPA to form uniform, wormhole-like mesopores. The success of pore templating with BTMSPA indicates that other bridged silanes with long hydrophilic chains may also be able to make uniform mesoporous materials by surfactant templating. However, templating by $C_{12}E_{10}$ is not effective. This illustrates that the interactions of the bridged silane with the template are very important in the success of the templating process. Thus, the inability of bridged silanes with long bridging polymethylene chains to make ordered mesoporous materials is likely to be due to both the flexibility of the organic bridge and poor co-assembly due to the hydrophobicity of the bridge.

Acknowledgments

This report is based on work partially supported by the National Science Foundation through CAREER grant number CTS-0348234. B.T. acknowledges partial support for this work through a Kentucky Research Challenge Trust Fund Fellowship.

References

[1] C.J. Brinker, G.W. Scherer, Sol–Gel Science: The Physics and Chemistry of Sol–Gel Processing, Academic Press, 1990.
[2] J.D. Wright, N.A.J.M. Sommerdijk, Sol–Gel Materials: Chemistry and Applications, Taylor & Francis Group, 2000.
[3] D.A. Loy, K.J. Shea, Chem. Rev. 95 (1995) 1431.
[4] P. Judeinstein, C. Sanchez, J. Mater. Chem. 6 (1996) 511.
[5] D.A. Loy, J.V. Beach, B.M. Baugher, R.A. Assink, Chem. Mater. 11 (1999) 3333.
[6] A. Stein, B.J. Melde, R.C. Schroden, Adv. Mater. 12 (2000) 1403.
[7] A. Sayari, S. Hamoudi, Chem. Mater. 13 (2001) 3151.
[8] C.T. Kresge, M.E. Leonowicz, W.J. Roth, J.C. Vartuli, J.S. Beck, Nature 359 (1992) 710.
[9] J.S. Beck et al., J. Am. Chem. Soc. 114 (1992) 10834.
[10] J.Y. Ying, C.P. Mehnert, M.S. Wong, Angew. Chem. Int. Ed. 38 (1999) 56.
[11] R.C. Hayward, P. Alberius-Henning, B.F. Chmelka, G.D. Stucky, Micropor. Mesopor. Mater. 44 (2001) 619.
[12] A. Monnier et al., Science 261 (1993) 1299.
[13] Q.S. Huo, D.I. Margolese, U. Ciesla, P.Y. Feng, T.E. Gier, P. Sieger, R. Leon, P.M. Petroff, F. Schüth, G.D. Stucky, Nature 368 (1994) 317.
[14] Q.S. Huo, D.I. Margolese, U. Ciesla, D.G. Demuth, P.Y. Feng, T.E. Gier, P. Sieger, A. Firouzi, B.F. Chmelka, F. Schüth, G.D. Stucky, Chem. Mater. 6 (1994) 1176.
[15] C. Boissiere, A. Larbot, C. Bourgaux, E. Prouzet, C.A. Bunton, Chem. Mater. 13 (2001) 3580.
[16] Y.L. Zub, I.V. Seregyuk, A.A. Chuiko, M. Jaroniec, M.O. Jones, R.V. Parish, S. Mann, Mendeleev Commun. (2001) 1.
[17] M.S. Rao, J. Gray, B.C. Dave, J. Sol–Gel Sci. Technol. 26 (2003) 553.
[18] K.J. Shea, D.A. Loy, Chem. Mater. 13 (2001) 3306.
[19] Y. Goto, S. Inagaki, Chem. Commun. 20 (2002) 2410.
[20] W.J. Hunks, G.A. Ozin, Chem. Mater. 16 (2004) 5465.
[21] W.J. Hunks, G.A. Ozin, Chem. Commun. 21 (2004) 2426.
[22] B. Tan, S.E. Rankin, J. Phys. Chem. B 2006, doi:10.1021/jp060376k.
[23] D. Kumar, K. Schumacher, C. du Fresne von Hohenesche, M. Grün, K.K. Unger, Colloid Surf. A 187&188 (2001) 109.
[24] C. Boissiere, A. Larbot, A. van der Lee, P.J. Kooyman, E. Prouzet, Chem. Mater. 12 (2000) 2902.
[25] M. Jaroniec, M. Kruk, J.P. Olivier, Langmuir 15 (1999) 5410.
[26] M. Kruk, M. Jaroniec, A. Sayari, Langmuir 13 (1997) 6267.
[27] P.J. Flory, J. Am. Chem. Soc. 63 (1941) 3083.
[28] L.V. Ng, P. Thompson, J. Sanchez, C.W. Macosko, A.V. McCormick, Macromolecules 28 (1995) 6471.
[29] V.W. Day, W.G. Klemperer, V.V. Mainz, D.M. Millar, J. Am. Chem. Soc. 107 (1985) 8262.
[30] C.S. Brevett, P.C. Cagle, W.G. Klemperer, D.M. Millar, G.C. Ruben, J. Inorg. Organomet. Polym. 1 (1991) 335.
[31] S.E. Rankin, L.J. Kasehagen, A.V. McCormick, C.W. Macosko, Macromolecules 33 (2000) 7639.
[32] J. Šefčík, S.E. Rankin, J. Phys. Chem. B 107 (2003) 52.
[33] Z. Zhang, Y. Tanigami, R. Terai, J. Non-Cryst. Solids 189 (1995) 212.
[34] D.A. Loy, B.M. Baugher, C.R. Baugher, D.A. Schneider, K. Rahimian, Chem. Mater. 12 (2000) 3624.
[35] L. Matejka, O. Dukh, J. Brus, W.J.S. Jr, B. Meissner, J. Non-Cryst. Solids 270 (2000) 34.
[36] D.A. Loy, J.P. Carpenter, T.M. Alam, R. Shaltout, P.K. Dorhout, J. Greaves, J.H. Small, K.J. Shea, J. Am. Chem. Soc. 121 (1999) 5413.
[37] K.S.W. Sing, D.H. Everett, R.A.W. Hual, L. Moscou, R.A. Pierottic, J. Rouquérol, T. Siemieniewska, Pure Appl. Chem. 57 (1985) 603.
[38] H.W. Oviatt Jr., K.J. Shea, J.H. Small, Chem. Mater. 5 (1993) 943.
[39] J.S. Beck, J.C. Vartuli, W.J. Roth, M.E. Leonowicz, C.T. Kresge, K.D. Schmitt, C.T.W. Chu, D.H. Olson, E.W. Sheppard, et al., J. Am. Chem. Soc. 114 (1992) 10834.
[40] B. Tan, S.E. Rankin, J. Phys. Chem. B 108 (2004) 20122.
[41] H.H.P. Yiu, C.H. Botting, N.P. Botting, P.A. Wright, Phys. Chem. Chem. Phys. 3 (2001) 2983.
[42] J. Yang, A. Daehler, G.W. Stevens, A.J. O'Connor, Adsorption of lysozyme and trypsin onto mesoporous silica materials, in: Nanotechnology In Mesostructured Materials, 2003. p. 775.
[43] A. Vinu, V. Murugesan, O. Tangermann, M. Hartmann, Chem. Mater. 16 (2004) 3056.
[44] P.T. Tanev, T.J. Pinnavaia, Science 267 (1995) 865.
[45] R.A. Assink, B.D. Kay, J. Non-Cryst. Solids 99 (1988) 359.